

Study of the multiplicity distributions of protons produced in proton-light nuclei collisions

Mais K. Suleymanov^{*1}, Amina M. Mammadova¹

¹Department of Matter Structure, Faculty of Physics, Baku State University, Baku, Azerbaijan

Received 19-Jun-2025; Accepted 05-Aug-2025

DOI: <https://doi.org/10.30546/209501.101.2025.2.03.015>

Abstract

This work investigates the multiplicity distributions of emitted protons produced in proton–nucleus collisions involving carbon, oxygen, and sodium nuclei at momenta of 4.2, 8.4, and 12.6 GeV/c. The study is based on simulated data obtained using the Dubna cascade-evaporation model. For each reaction, 10,000 events were analyzed. The results show that the proton multiplicity distributions exhibit three characteristic regions corresponding to the values: $n \approx 0-4$, $n \approx 5-7$, and $n \geq 8$. We assume that the region $n \approx 0-4$ corresponds to peripheral collisions, $n \approx 5-7$ to semi-central collisions, and $n \geq 8$ to central collisions. The results confirm that the degree of collision centrality is directly related to the number of emitted protons. In peripheral collisions, the interaction involves only the outer layers of the nucleus, resulting in a smaller number of emitted particles. In central collisions, by contrast, the interaction affects a larger portion of the nucleus, leading to a sharp increase in the number of emitted protons.

Keywords: Proton–nucleus collisions, multiplicity distributions, collision centrality, energy dependence, target-mass dependence.

PACS Numbers: 25.40.Ep; 25.70.-z

1. Introduction

The study of the characteristics of protons emitted as a result of high-energy collisions involving light nuclei plays a key role in exploring the dynamics of particle interactions. These collisions represent an intermediate stage between proton–

^{*}Corresponding author – Tel.: (+994) 50 531 43 88

e-mail: mais.suleymanov@bsu.edu.az; ORCID ID: 0000-0003-4231-0480

proton and nucleus–nucleus interactions, enabling a deeper understanding of collision mechanisms. They are essential for studying phenomena such as the collective behavior of nuclear matter and the formation of its ultra-dense and overheated states [1]. These questions are currently being actively investigated in experiments at the Large Hadron Collider [2].

To date, a significant number of studies have been devoted to proton–nucleus interactions [3]. These investigations have provided the fundamental characteristics of such events, as well as the properties of particles formed as a result of the interactions. Various theoretical models have been developed to interpret the results, along with software packages based on these models [4]. However, with the emergence of new experimental and theoretical data, these models continue to evolve and are being refined with additional mechanisms.

One of the most widely used models for describing such interactions is the Dubna version of the cascade–evaporation model [5]. Its application has yielded several important results in the study of proton–nucleus collisions, and work on improving this model is ongoing [6].

Proton–nucleus collisions provide deeper insight into the structure and properties of nuclear matter at high energies, as well as the mechanisms of particle production under such conditions. Research in this area has shown that:

- Proton–nucleus interactions occur in two key stages: a cascade stage (based on sequential nucleon–nucleon collisions) and an evaporation stage (particle emission during nuclear relaxation).
- The reaction mechanism depends on the energy of the incident proton: at low energies (up to 200 MeV), direct interaction processes dominate, while at high energies, cascade and collective effects prevail.
- In high-energy proton collisions (>1 GeV) with nuclei, a large number of nucleons are ejected — a process known as spallation.
- A broad spectrum of nuclear residues is produced, varying in mass, charge, and energy.
- The distribution of emitted particles by energy and emission angle depends on both the mass of the target nucleus and the energy of the incoming proton.
- Optical potential models successfully describe both elastic and inelastic scattering.
- At high energies (>10 GeV), proton–nucleus collisions result in the production of not only nucleons but also mesons, hyperons, and pions.
- The effective cross section of particle production is well described by quark–gluon models.
- These results remain relevant and require continued investigation and refinement.

The present study is dedicated to this problem. Its main objective is to investigate the changes in the multiplicity properties of proton–nucleus interactions as a function of the incident proton energy and the mass of the target nucleus.

2. Method

In the present study, the multiplicity distribution spectra of protons produced as a result of proton collisions with carbon (^{12}C), oxygen (^{16}O), and sodium (^{23}Na) nuclei at incident proton momenta of 4.2, 8.4, and 12.4 GeV/c were analyzed. For each reaction, 10,000 events were examined. The obtained data are compared with similar data from the experiments reported in [7].

3. Results

In Using the method described above, multiplicity distribution spectra of protons produced in collisions of protons with carbon (^{12}C), oxygen (^{16}O), and sodium (^{23}Na) nuclei were obtained.

Figure 1 shows the proton multiplicity distributions for the reactions $p+O \rightarrow$ at three different values of the incident proton momentum (p) in the laboratory frame of reference. Analysis of the graphs indicates that in the region of peripheral collisions (the main characteristics of peripheral, semi-central, and central collisions are presented in Table 1), for $n \approx 0-4$, the distributions are nearly identical both quantitatively and qualitatively—that is, no significant energy dependence is observed.

In semi-central collisions, at $n \approx 5-7$, a quantitative difference emerges at a momentum of 4.2 GeV/c, indicating the onset of the influence of the incident proton's energy. In central collisions ($n \approx 8-12$), the distribution curves diverge significantly at all three momentum values, which points to an increased dependence on the energy of the incident proton ($E = \sqrt{p^2 c^2 + m^2 c^4}$, where c is the speed of light and m is the proton mass).

Table 1. Main Characteristics of Peripheral, Semi-Central, and Central Collisions

Parameter	Peripheral Collision	Semi-Central Collision	Central Collision
Impact parameter (b)	$b \approx R_1 + R_2$ (R_1 and R_2 are the radii of the colliding objects)	$0 < b < R_1 + R_2$	$b \approx 0$
Interaction zone	Outer layers of the colliding objects	Moderate overlap of the nuclei	Full overlap of the nuclei

Analysis of the behavior of proton multiplicity distributions in the reactions $p + O \rightarrow$ as a function of the incident proton energy leads to the following conclusions: in peripheral collisions, the influence of energy is minimal, as the interaction occurs primarily with the outer nucleons, and cascade processes have little effect on the distribution of emitted particles; in semi-central collisions, both outer and inner nucleons are involved, resulting in a more pronounced energy dependence of the dis-

tributions; in central collisions, the entire nuclear structure participates in the interaction, cascade processes are significantly intensified, and the influence of the incident proton's energy becomes most evident, determining the character of the emitted particle distribution.

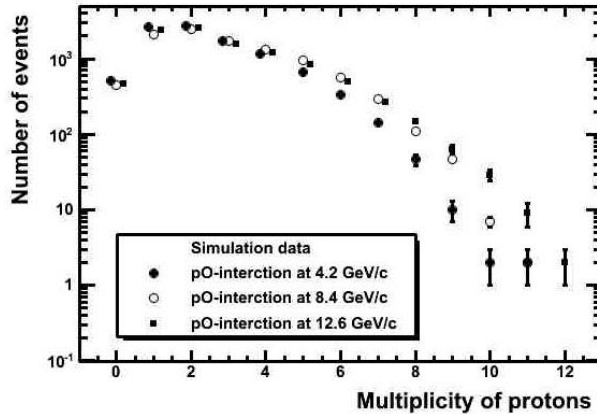


Fig. 1. Distribution of protons emitted in the reactions $p + O \rightarrow$ at three different proton energies in the laboratory frame: 4.2, 8.4, and 12.6 GeV/c.

Figures 2–3 show the distributions of protons emitted in the reactions $p + C \rightarrow$ (Fig. 2) and $p + Na \rightarrow$ (Fig. 3) at three different values of the proton momentum in the laboratory frame: 4.2, 8.4, and 12.6 GeV/c. From the presented data, it follows that, similar to the case of the $p + O \rightarrow$ reactions, in the peripheral region ($n \approx 0-4$), the distributions coincide both quantitatively and qualitatively, meaning no energy dependence is observed. In semi-central collisions ($n \approx 5-7$), a quantitative difference is noted at a momentum of 4.2 GeV/c, indicating the emergence of energy dependence. In the central collision region ($n \approx 8-12$), the distribution curves diverge noticeably for all three momentum values, which indicates a strengthening of the energy dependence.

Thus, it can be concluded that, with a change in the target nucleus mass, the general pattern of the multiplicity distributions of protons emitted in the reactions $p + O \rightarrow$, $p + C \rightarrow$, and $p + Na \rightarrow$ remains unchanged with variation in the energy of the incoming proton.

For ease of comparison and to further confirm the aforementioned results, Figures 4, 5, and 6 present the multiplicity distributions of emitted protons in events with different target nucleus masses at fixed values of the incident proton momentum: 4.2, 8.4, and 12.6 GeV/c, respectively.

From the presented figures, the following observations can be made:

- At a momentum of 4.2 GeV/c, as the number of protons increases in the region of $n \approx 0$ – (peripheral collisions), the proton multiplicity distributions for different

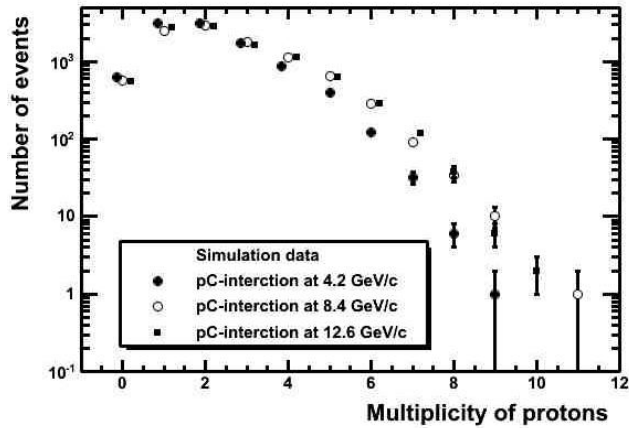


Fig. 2. Distribution of protons emitted in the reactions $p + C \rightarrow$ at three different proton energies in the laboratory frame: 4.2, 8.4, and 12.6 GeV/c.

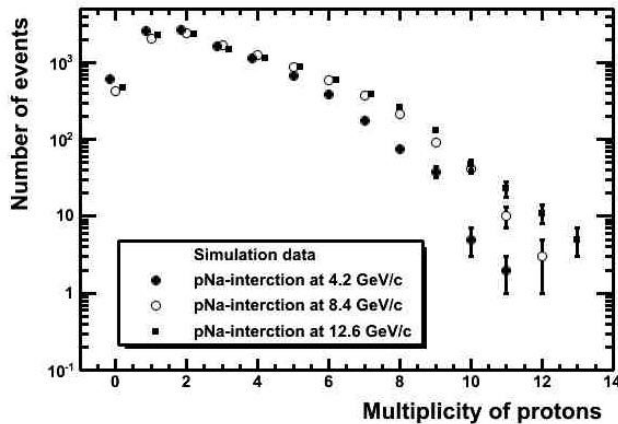


Fig. 3. Distribution of protons emitted in the reactions $p + Na \rightarrow$ at three different proton energies in the laboratory frame: 4.2, 8.4, and 12.6 GeV/c.

target nucleus masses coincide. In the region $n \approx 5-8$ (semi-central collisions), deviations are observed for carbon targets, and at $n \geq 8$ (central collisions), the deviations become more pronounced and are evident for all target masses.

- At a momentum of 8.4 GeV/c, a similar pattern is observed: in the region $n \approx 0-4$, the proton multiplicity distributions coincide for different target nucleus masses; in the region $n \approx 5-7$, deviations appear for carbon targets, and at $n \geq 8$, the deviations intensify and are observed for all target masses.
- At a momentum of 12.6 GeV/c, the trends remain similar to those at 4.2 and 8.4 GeV/c: in the region $n \approx 0-4$, the proton multiplicity distributions coincide

for different target nucleus masses; in the region $n \approx 5-7$, deviations are noted for carbon targets, and at $n \geq 8$, the deviations become stronger and are observed across all target masses.

We assume the following:

- The region $n \approx 0-4$ corresponds to peripheral collisions, in which the interaction involves only a minimal portion of the target nucleus mass.
- The region $n \approx 5-7$ reflects semi-central collisions, where the number of participating nucleons increases.
- The region $n \geq 8$ is associated with central collisions, characterized by the maximum number of interacting nucleons in the target nucleus.

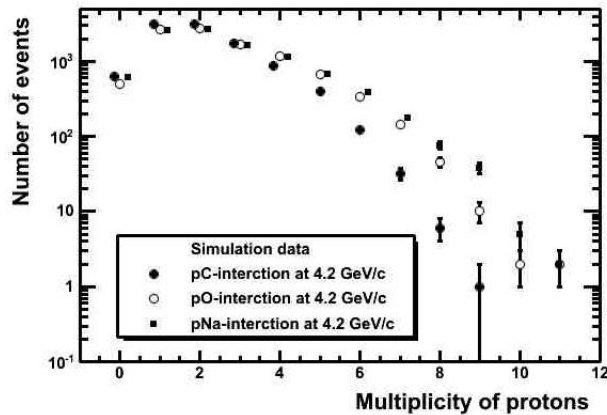


Fig. 4. Distribution of protons emitted in pC, pO, and pNa reactions at a proton momentum of 4.2 GeV/c in the laboratory frame.

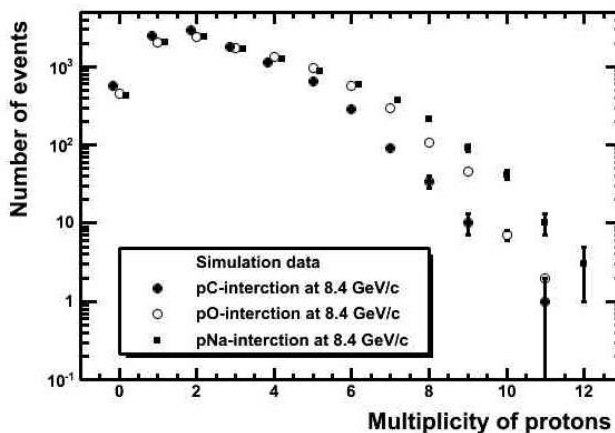


Fig. 5. Distribution of protons emitted in pC, pO, and pNa reactions at a proton momentum of 8.4 GeV/c in the laboratory frame.

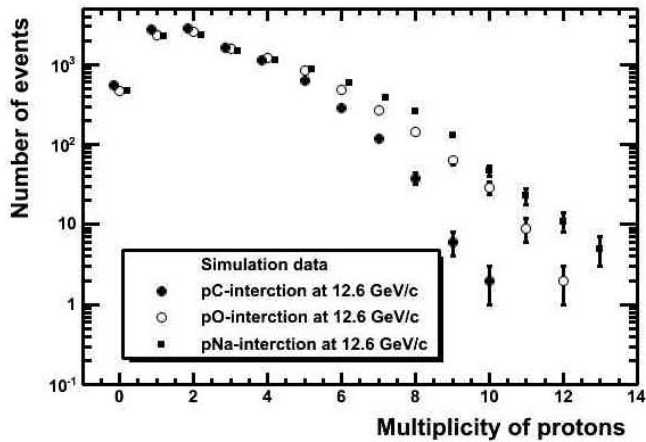


Fig. 6. Distribution of protons emitted in pC, pO, and pNa reactions at a proton momentum of 12.6 GeV/c in the laboratory frame.

Thus, three characteristic regions can be distinguished in the behavior of the proton multiplicity distributions: $n \approx 0-4$, $n \approx 5-7$, and $n \geq 8$. This confirms that the degree of collision centrality is directly related to the number of emitted protons (n). In peripheral collisions, the interaction affects only the outer layers of the nucleus, resulting in a smaller number of emitted particles, whereas in central collisions, a larger part of the nucleus is involved, leading to a significant increase in the number of emitted protons.

In [7], experimental data are presented on proton multiplicities obtained in interactions of protons with a momentum of 4.2 GeV/c with carbon nuclei using a 2-meter propane bubble chamber installed at the Laboratory of High Energies (Joint Institute for Nuclear Research, Dubna). The data are categorized by the degree of collision centrality. As a criterion for the centrality degree, the Q parameter is used, defined for each individual event as the difference between the multiplicities of positively and negatively charged particles, excluding the multiplicity of evaporated protons with a momentum below 0.3 GeV/c. It was shown that with increasing Q , the multiplicity of participating protons emitted from the target nucleus increases significantly, while the average multiplicity of evaporated protons decreases sharply. The experimental results were compared with theoretical calculations performed within the framework of the cascade-evaporation model and a modified FRITIOF model, which takes into account non-nucleonic degrees of freedom in nuclei.

4. Conclusion

The study of proton multiplicities produced in collisions of protons with carbon, oxygen, and sodium nuclei at momenta of 4.2, 8.4, and 12.6 GeV/c, carried out

based on simulated data obtained using the Dubna cascade-evaporation model, revealed the presence of three characteristic regions in the distributions of emitted protons. These regions correspond to the following values: $n \approx 0-4$, $n \approx 5-7$, and $n \geq 8$.

We assume that:

- The region $n \approx 0-4$ corresponds to peripheral collisions, where the interaction affects only the outer layers of the nucleus.
- The region $n \approx 5-7$ is typical for semi-central collisions, in which the involved mass of the nucleus increases.
- The region $n \geq 8$ corresponds to central collisions, where a significant portion of the nucleus participates in the interaction.

The obtained results confirm that the degree of collision centrality is directly related to the number of emitted protons (n). In peripheral collisions, proton emission is minimal due to weak interaction with the nucleus, whereas in central collisions, involvement of a larger part of the nucleus leads to a sharp increase in the number of emitted particles.

References

- [1] Blaizot, J.-P. (2001). The physics of the quark-gluon plasma: Recent advances. *Nuclear Physics A*; Kolb, P. F., & Heinz, U. (2004). Relativistic hydrodynamics and heavy-ion collisions. In *Quark-Gluon Plasma 3*; Shen, H., et al. (1998). Equation of state of hot and dense nuclear matter: From supernovae to neutron stars. *Progress of Theoretical Physics Supplement*; Prakash, M., et al. (1997). High density matter in neutron stars and supernovae. *Physics Reports*; Greiner, C., & Rischke, D. H. (1996). Quark matter and the equation of state for dense baryonic matter. *Physics Reports*; McLerran, L. (1986). Phase transitions in hot and dense nuclear matter. *Reviews of Modern Physics*.
- [2] Evans, L., & Bryant, P. (2008). The Large Hadron Collider: A marvel of technology. *Journal of Instrumentation*, 3(08), S08001.
<https://doi.org/10.1088/1748-0221/3/08/S08001>
- [3] Feshbach, H., Kerman, A., & Koonin, S. (1980). Proton-nucleus scattering and the nuclear optical potential. *Annals of Physics*. [https://doi.org/10.1016/0003-4916\(80\)90151-6](https://doi.org/10.1016/0003-4916(80)90151-6); Hodgson, P. E. (1971). Measurements of proton-nucleus cross sections at intermediate energies. *Reports on Progress in Physics*. <https://doi.org/10.1088/0034-4885/34/2/303>; Hüfner, J., & Thoma, M. (1992). High-energy proton-nucleus collisions: From Fermi motion to quark-gluon dynamics. *Physics Reports*. [https://doi.org/10.1016/0370-1573\(92\)90147-G](https://doi.org/10.1016/0370-1573(92)90147-G); Hill, D. L., & Wheeler, J. A. (1953). Experimental study of proton scattering on light nuclei. *Physical Review*, 89, 1102. <https://doi.org/10.1103/PhysRev.89.1102>; ALICE Collaboration. (2013). Proton-nucleus collisions at the LHC: Insights into initial state effects. *Journal of High Energy Physics*, 2013(2), 073. [https://doi.org/10.1007/JHEP02\(2013\)073](https://doi.org/10.1007/JHEP02(2013)073); Gaisser, T. K., & Engel, R. (1998). Proton-nucleus interactions and their role in cosmic ray physics. *Astroparticle Physics*. [https://doi.org/10.1016/S0927-6505\(98\)00044-2](https://doi.org/10.1016/S0927-6505(98)00044-2)

- [4] Osterfeld, F. (1985). The optical model in nuclear and particle physics. *Reviews of Modern Physics*. <https://doi.org/10.1103/RevModPhys.57.689>; Xu, W. H., & Brown, B. A. (1994). Global optical potential for proton-nucleus scattering at intermediate energies. *Physics Letters B*. [https://doi.org/10.1016/0370-2693\(94\)90015-9](https://doi.org/10.1016/0370-2693(94)90015-9); Pandharipande, V. R., & Wiringa, R. B. (1979). Microscopic theory of proton scattering from spherical nuclei. *Nuclear Physics A*. [https://doi.org/10.1016/0375-9474\(79\)90514-5](https://doi.org/10.1016/0375-9474(79)90514-5); Glauber, R. J. (1959). Proton-nucleus collisions in the Glauber model. *Physical Review*, 116, 231. <https://doi.org/10.1103/PhysRev.116.231>; Weinberg, S. (1991). Effective field theory for proton-nucleus interactions. *Physical Review Letters*, 67, 3473. <https://doi.org/10.1103/PhysRevLett.67.3473>; Bang, J. M., & Gareev, F. A. (1973). Coupled-channels approach to proton-nucleus reactions. *Nuclear Physics A*. [https://doi.org/10.1016/0375-9474\(73\)90249-2](https://doi.org/10.1016/0375-9474(73)90249-2); Hodgson, P. E. (1971). Quantum-mechanical studies of proton-induced reactions on nuclei. In *Advances in Nuclear Physics*. https://doi.org/10.1007/978-1-4612-6370-4_1; Khoa, D. T., & Than, H. S. (1997). Nucleon-nucleus scattering and shell model effects. *Physics Letters B*. [https://doi.org/10.1016/S0370-2693\(97\)01202-4](https://doi.org/10.1016/S0370-2693(97)01202-4)
- [5] Toneev, V. D., & Gudima, K. K. (1986). Cascade models of nuclear reactions: Review and perspectives. *Physics of Atomic Nuclei*. <https://doi.org/10.1142/S0218301386000054>; Sobolevsky, N. M., & Toneev, V. D. (1971). Cascade-exciton model of nuclear reactions. *Physics Letters B*. [https://doi.org/10.1016/0370-2693\(71\)90319-7](https://doi.org/10.1016/0370-2693(71)90319-7); Toneev, V. D., & Gudima, K. K. (1973). Cascade-exciton model for high-energy nuclear reactions. *Nuclear Physics A*. [https://doi.org/10.1016/0375-9474\(73\)90209-7](https://doi.org/10.1016/0375-9474(73)90209-7); Gudima, K. K., & Mashnik, S. G. (1990). Proton-induced reactions on nuclei in the framework of the cascade-exciton model. *Nuclear Instruments and Methods in Physics Research B*. [https://doi.org/10.1016/0168-583X\(90\)90539-Y](https://doi.org/10.1016/0168-583X(90)90539-Y); Mashnik, S. G., & Toneev, V. D. (1998). Fragmentation of heavy nuclei in the Dubna cascade model. *Physical Review C*. <https://doi.org/10.1103/PhysRevC.58.1503>; Mashnik, S. G., & Prael, R. E. (2003). MCNPX simulations based on the Dubna cascade-exciton model. *Nuclear Science and Engineering*. <https://doi.org/10.13182/NSE03-A342>
- [6] Gudima, K. K., Mashnik, S. G., & Toneev, V. D. (1983). CEM of nuclear reactions: Development and applications. *Nuclear Science and Engineering*. <https://doi.org/10.13182/NSE83-A23657>; Mashnik, S. G., Sierk, A. J., & Gudima, K. K. (1994). Dubna cascade-exciton model: New developments and applications. *Journal of Nuclear Physics*. <https://doi.org/10.1088/0954-3899/20/9/002>; Mashnik, S. G., & Toneev, V. D. (1997). Improved cascade-exciton model for spallation reactions. *Physics of Particles and Nuclei*. <https://doi.org/10.1134/1.953069>; Mashnik, S. G., & Sierk, A. J. (2000). Improved version of the cascade-exciton model for nuclear reactions. Los Alamos National Laboratory Report. Retrieved from <https://lanl.gov>
- [7] Uzhinskii, V. V., et al. (2003). *Physics of Atomic Nuclei*, 66(5), 836–846.